Impaired dendritic-cell homing in vivo in the absence of Wiskott-Aldrich syndrome protein

Sofia de Noronha, Samantha Hardy, Joanna Sinclair, Michael P. Blundell, Jessica Strid, Oliver Schulz, Jörg Zwirner, Gareth E. Jones, David R. Katz, Christine Kinnon, and Adrian J. Thrasher

Regulated migration and spatial localization of dendritic cells (DCs) are critical events during the initiation of physiologic immune responses and maintenance of tolerance. Here we have used cells deficient in the Wiskott-Aldrich syndrome protein (WASp) to demonstrate the importance of dynamic remodeling of the actin cytoskeleton for these trafficking processes to occur in vitro and in vivo. On fibronectin-coated surfaces, WASp-null immature murine DCs exhibited defects both of attachment and detachment, resulting in impaired net translocation compared with normal cells. The chemokinetic response to CCL21, which is critical for normal lymphatic trafficking, was also abrogated in the absence of WASp. In vivo in both fluorescein isothiocyanate (FITC) and oxazolone contact hypersensitivity models, WASp-null Langerhans cell (LC) migration was compromised, as judged by exit from the skin as well as by homing to the draining lymph node (LN). Furthermore, following systemic challenge with lipopolysaccharide (LPS) or toxoplasma-derived antigen, WASp-null DCs showed incomplete redistribution to T-cell areas in the spleen. Instead, they were retained ectopically in the marginal zone. DC trafficking in vivo is therefore dependent on a normally regulated actin cytoskeleton, which performs an essential function during maintenance of physiologic immunity and when disturbed may contribute significantly to the immunopathology of Wiskott-Aldrich Syndrome. (Blood. 2005;105:1590-1597)

Introduction

Dendritic cells (DCs) are highly motile bone marrow–derived antigen-presenting cells (APCs). They have specialized migratory and homing properties that allow them both to initiate primary immune responses and to induce tolerance.[1,2] In lymphoid organs they are present as interdigitating cells in the white pulp of the spleen and in the paracortex of lymph nodes (LNs) where they are able to capture incoming foreign antigen from blood or lymph, respectively. In nonlymphoid tissues DCs act as sentinels of injury and patrol for the presence of foreign antigens and pathogens. Upon capture they migrate to draining secondary lymphoid tissue during which time they mature and develop the capacity to stimulate antigen specific T cells.

The migration and spatial localization of DCs are controlled by numerous extrinsic factors, including chemokine family members to which they are responsive through maturation and localization-dependent mechanisms.[3-7] The physical motility of cells and anchorage in specific tissues is, however, ultimately dependent on the regulated dynamics of the actin cytoskeleton, which determines the response of cells to chemokine gradients and enables purposeful movement through the sequential process of leading-edge protrusion, attachment, and tail retraction.[8] The molecular control of this highly coordinated activity is orchestrated by Rho family guanosine triphosphatases (GTPases), the best characterized of which are Cdc42, Rac1/2, and RhoA, and their downstream effectors.[9] In hematopoietic cells, a key effector for Cdc42 is the Wiskott-Aldrich syndrome protein (WASp). WASp is a 502–amino acid member of a conserved family of proteins that participate in the organization of actin polymerization primarily through activation of the actin-related protein (Arp2/Arp3) complex.[10-12] Interference in these signaling pathways results in multiple cytoskeletal defects in DCs, including the failure to form normal membrane projections and specialized structures known as podosomes, which form behind the leading edge of motile cells.[13-16] Podosomes concentrate β2 integrins around an actin core and, although their function has not been clearly identified, are responsible for tight adhesion of cells to intercellular adhesion molecule-1 (ICAM-1) and possibly junctional adhesion molecule-A (JAM-A).[17-19] Furthermore, they are highly dynamic with a turnover of minutes, providing a migrating cell with a mechanism for rapid attachment and detachment, and with localized anchorage points that could facilitate traverse of endothelial barriers in particular.

Wiskott-Aldrich syndrome (WAS) is characterized by microthrombocytopenia, immunodeficiency, eczema, and autoimmunity.[12] The pathophysiology of WAS relates to defective polymerization of

From the Molecular Immunology Unit, Institute of Child Health, London, United Kingdom; the Immunobiology Unit, Institute of Child Health, London, United Kingdom; the Immunobiology Laboratory, Cancer Research United Kingdom, Lincoln's Inn Fields Laboratories, London, United Kingdom; the Department of Immunology, Georg-August-University Göttingen, Germany; the Randall Centre for Molecular Mechanisms of Cell Function, King's College London, United Kingdom; the Department of Immunology, University College London, Windeyer Institute, United Kingdom; and the Department of Clinical Immunology, Great Ormond Street Hospital NHS Trust, London, United Kingdom.

Submitted June 18, 2004; accepted October 3, 2004. Prepublished online as *Blood* First Edition Paper, October 19, 2004; DOI 10.1182/blood-2004-06-2332.

Supported by the European Union (FP5 grant QLG1-1999-01090) (S.H.) and the Child Health Research Appeal Trust of the Institute of Child Health (S.de N.).

A.J.T. is a Wellcome Trust Senior Clinical Fellow.

The online version of the article contains a data supplement.

Reprints: Adrian Thrasher, Molecular Immunology Unit, Institute of Child Health, 30 Guilford St, London, WC1N 1EH, United Kingdom; e-mail: a.thrasher@ich.ucl.ac.uk.

The publication costs of this article were defrayed in part by page charge payment. Therefore, and solely to indicate this fact, this article is hereby marked "advertisement" in accordance with 18 U.S.C. section 1734.

monomeric actin in hematologic cells, although the predominating mechanisms that result in dysregulated immunity have not been clearly identified. Almost certainly the complex phenotype results from multiple defects of cell function and receptor signaling.[20-26] However, defects of migration identified in myeloid and T cells in vitro, and stem cells in vivo,[27-31] all support the hypothesis that many of the immunologic consequences of WASp deficiency arise from abnormal cell homing and spatial localization.

In previous studies, we and others have characterized profound defects of WAS patient DC migration in vitro, including failure to achieve normal polarization and effective translocation. From these observations, it seemed likely that DC trafficking abnormalities in vivo would contribute in a significant way to the immunologic dysregulation of WAS. For example, the failure of DCs to localize appropriately within secondary lymphoid tissue, in the context of normal activation in terms of cytokine production or up-regulation of cell surface ligands, may be sufficient to initiate ectopic and uncontrolled T-cell responses. Similarly, trapping of DCs at peripheral sites following activation may result in the formation of inflammatory foci. These hypothetical consequences of WASp deficiency on DC traffic are difficult to confirm in vivo in patients with WAS. We have therefore used a murine model of WASp deficiency to demonstrate abnormalities of DC trafficking in vivo.

Materials and methods

Mice

WASp-deficient mice (WASp-null, sv129 background) generated by gene targeting were a gift from Drs S. Snapper and F. Alt (Harvard Medical School, Boston, MA).[21] The mice were bred and maintained in sterile isolators. Control mice were also from a sv129 background (purchased from Harlan, Leicester, United Kingdom). All animal experiments were approved by the relevant regulatory authorities.

Microbial-derived stimuli

Soluble tachyzoite antigen (STAg) was prepared from tachyzoites of the RH 88 strain of *Toxoplasma gondii*, as previously described (a gift from C. Reis e Sousa).[32] STAg was administered to mice at a dose of 10 μg per mouse. Lipopolysaccharide (LPS) from *Escherichia coli* 026:B6 (Sigma, Poole, United Kingdom) was used at 1 μg per mouse. Each stimulus was dissolved in 200 μL and injected intraperitoneally. Control mice received the same volume of phosphate-buffered saline (PBS) only. All animals were killed at the same time. Preliminary experiments showed that the response to STAg of the sv129 strain was comparable to that of other strains previously investigated.

Isolation of bone marrow–derived dendritic cells

Bone marrow–derived DCs (BMDCs) were prepared as described[33] with some modifications. Bone marrow (BM) from femora and tibiae of mice was distributed into Falcon flasks (BD Biosciences, Bedford, MA) to a final concentration of approximately 1 to 2×10^6cells/mL in RPMI 1640 Glutamax-1 with HEPES (*N*-2-hydroxyethylpiperazine-*N*′-2-ethanesulfonic acid, 25mM; Gibco Life Technologies, Paisley, United Kingdom) supplemented with 10% fetal calf serum (Autogen Bioclear, Wiltshire, United Kingdom) and 10 000 IU/mL penicillin and streptomycin (Gibco Life Technologies). Granulocyte-macrophage colony-stimulating factor (GM-CSF) was in the form of a supernatant derived from a plasmacytoma cell line transfected with an expression vector containing the polymerase chain reaction (PCR)–derived mouse *GM-CSF* gene[34] and used at 5% of the conditioned medium (CM). Alternatively recombinant GM-CSF (Insight Biotechnology, Middlesex, United Kingdom) was used at 25 ng/mL. On day 3 growth media was replenished. Cells were then harvested on day 8 by centrifugation.

BMDC phenotyping

On day 7 to 8 the floating cell fraction of the BMDC culture was extracted and washed with PBS. Cells were stained with a panel of antibodies including CD11c-fluorescein isothiocyanate (FITC; clone HL3), unlabeled I-A^b supernatant, unlabeled CD80 (clone 1G10), unlabeled DEC205 supernatant, and a monoclonal antibody specific for mouse CCR7,[35] in FACS (fluorescence activated cell sorting) washing buffer (FWB). After 45 minutes, cells were washed twice in FWB and stained with FITC-labeled anti-rat (for unlabeled antibodies). After 30 minutes cells were washed again and visualized by flow cytometry using a Beckman Coulter FACS (High Wycombe, United Kingdom).

Cell motility studies

BMDCs (10^5), prepared as outlined in "BMDC phenotyping," were plated on fibronectin (FN)–coated 13-mm coverslips and allowed to adhere for 2 hours at 37°C/5% CO_2. Dunn chambers (Weber Scientific, Hamilton, NJ) were assembled as previously described.[14,36] Inner and outer wells of the Dunn chambers were filled with CM supplemented with GM-CSF. For each experiment 2 Dunn chambers were run in parallel. Dunn chambers were maintained at 37°C/5% CO_2 on a microscope stage. Using an inverted microscope (Olympus, Southall, United Kingdom) cells located on the viewing bridge of the chamber were visualized using a 20 ×/0.4 objective lens with a 1.5 × optivar. Images were acquired using Sony video cameras (CCD-IRIS) and either recorded on to a Betacam SP recorder (Sony, Berkshire, United Kingdom) or on to a personal computer (PC) using AQM:AMVS (Kinetic Imaging, Nottingham, United Kingdom). The camera was set to acquire 1 frame every 10 minutes over a 5-hour period. The processed sequences were then replayed as a movie. To test cell motility to CCL21, BMDCs were isolated as described earlier but with addition of LPS at 0.5 μg/mL on day 6, and with selection of $CD11c^+$ cells using magnetic activated cell sorting (MACS) microbeads (clone N418; Miltenyi Biotec, Surrey, United Kingdom) according to manufacturer's instructions on day 7. Matured BMDCs were similar in phenotype to the pre-LPS–treated cells with regard to $CD11c^+$ and I-A^{b+} expression. Dunn chambers and the outer well of the chamber were either filled with CM or CM supplemented with recombinant murine CCL21 (at 100 ng/mL; R&D Systems, Abingdon, United Kingdom). Dunn chambers were maintained at 37°C on a microscope stage (Zeiss Axiovert 135; Zeiss, Hertfordshire, United Kingdom), and cell motility was recorded using a 10 ×/0.25 objective lens for the next 5 hours (the stimulation period) using a Hamamatsu digital camera (C4742-95) and Improvision Openlab software version 3 (Improvision, Coventry, United Kingdom). Images were first analyzed as described previously[28,37] and processed using Mathematica notebooks version 4 (Wolfram Research, Champaign, IL), which provide detailed statistical data on the rates of leukocyte movement and related migration parameters.

FITC sensitization and detection in LNs

Preliminary experiments examined the amount of FITC required for detection, the solvent requirements, and different time points. On the basis of these results, 0.5% FITC was dissolved in a 1:1 (vol:vol) acetone/dibutyl phthalate mixture immediately before application to give a final concentration of 5 mg/mL. Mice were painted on the abdomen with 0.2 mL FITC. At 4 hours and 18 hours, inguinal LNs were removed, and cell suspensions were obtained after digestion with Liberase CI (Boehringer Mannheim, Mannheim, Germany) and DNAse I (Roche, Basel, Switzerland) for 20 minutes at 37°C. Next, cells were washed twice in PBS/5 mM ethylene diamine tetra-acetic acid (EDTA), and the resultant LN cell suspension was depleted of B cells and T cells using anti-IgG (immunoglobulin G) and anti-Thy.1 Dynabeads (product nos. 114.03 and 114.01; Dynal, Oslo, Norway). LNs were pooled from 2 mice for each category, because insufficient cells could be harvested from individual nodes. Preliminary experiments showed that FITC was not associated with $F4/80^+$ cells, supporting the notion that cells migrating to LNs with FITC are DCs, as has been reported previously.[38] The remaining cells were stained with biotinylated I-A^b (clone KH74) for 1 hour followed by streptavidin–phycoerythrin (PE) for 30 minutes. After gating on live cells, events (30 000-50 000) were collected using Beckman Coulter FACS machine (High Wycombe, United Kingdom).

Oxazolone sensitization and immunohistochemical staining of Langerhans cells

Groups of 3 mice were sensitized by application of 15 μL 1% oxazolone in acetone/olive oil (AOO; 4/1) to the whole surface of each mouse ear. Control mice received AOO only. The ears were removed after 4 hours to quantify the number of Langerhans cells (LCs) before and after sensitization, where a drop in LC number of cells indicated emigration from the skin. The method of LC quantification followed has been described previously.[39] Briefly, ears were excised and split into dorsal and ventral halves using fine forceps. Dorsal halves were incubated in 0.02 M EDTA at 37°C for 90 minutes to allow separation of the epidermis and dermis. Epidermal sheets were peeled away from the dermis carefully, washed twice in PBS, fixed in acetone (−20°C, 20 minutes), and washed again. The sheets were incubated with biotin–anti-mouse I-A^b (5 μg/mL in PBS with 0.1% bovine serum albumin [BSA], 60 minutes, at room temperature), washed 3 times, and then incubated for an additional 45 minutes with streptavidin-FITC. After further washes the epidermal sheets were mounted in Citifluor AF1 Mountant Medium (Citifluor, Leicester, United Kingdom). LCs were counted on a Zeiss Axiophot2 fluorescent microscope (Zeiss) in 10 fields in the central portion of the ear using a calibrated grid eyepiece in a 40 ×/0.75 objective lens. Results were expressed as the mean plus or minus standard deviation of the number of LCs per square millimeter of epidermis. LCs were imaged on the same microscope and processed using Improvision Openlab software version 3 (Improvision, Coventry, United Kingdom).

Immunohistochemistry

Spleens were cut transversely through the hilus, and a slice was rapidly frozen in tissue mounting gel in a dry ice/isopentane bath. The rest of the spleen was used for flow cytometric analysis. Cryosections (7 μm) were cut onto poly-L-lysine–coated slides (BDH, Poole, United Kingdom) and stored at −70°C. Slides were thawed and fixed in acetone at room temperature for 10 minutes and rehydrated in phosphate-buffered saline (PBS). Endogenous peroxidase was blocked with 0.3% H_2O_2. Sections were stained with a biotin-conjugated hamster anti-mouse CD11c antibody (clone HL3) and unconjugated rat anti-mouse CD19 (clone 1D3) in 0.5% Biorad blocker (BioRad Laboratories, Hercules, CA) at a concentration of 5 μg/mL for 1 to 2 hours at room temperature. Antibody-treated sections were washed 5 times in PBS and then incubated with a streptavidin-biotinylated peroxidase complex (Vectastain ABC kit; Vector Laboratories, Peterborough, United Kingdom) for 30 minutes at room temperature. Peroxidase activity was visualized using Immunopure Metal Enhanced DAB (diaminobenzidine) substrate Kit (Pierce, Rockford, IL) and washed again in PBS. To determine CD19 expression, sections were stained with biotin-conjugated mouse $F(ab')_2$ anti-rat IgG (1.4 μg/mL; Jackson ImmunoResearch Laboratories, West Grove, PA). After repeated washing, sections were incubated with a streptavidin-biotinylated phosphatase complex (Vectastain, ABC-AP kit) and developed with vector-red substrate (both Vector Laboratories). The tissue was counterstained with methyl green, and after dehydrating, the tissue was mounted in 1,3-diethyl-8-phenylxanthine (DPX) mountant (BDH). All antibodies were purchased from Pharmingen (San Diego, CA) unless otherwise stated. Spleen sections were imaged using a Zeiss Axioplan2 light microscope (Zeiss) equipped with 10 ×/0.3 and 20 ×/0.5 objective lenses. Images were captured with Progress version 5 plugin (Jenoptik, Jena, Germany) for Adobe Photoshop 6.0 software (Adobe Systems, Uxbridge, United Kingdom).

Flow cytometric analysis of STAg-stimulated DCs

Spleen cell suspensions were obtained as described earlier in "FITC sensitization and detection in LNs." Spleen cells were fixed in 1% paraformaldehyde in PBS for 10 minutes, washed, and kept overnight in FWB containing PBS, 0.5% BSA, and 0.01% NaN_3 at 4°C. The next day cells at 5 to 10 × 10^6/500 μL were blocked with anti-mouse Fcγ III/II receptor (clone 2.4G2) at 5 μg/mL for 5 minutes and then stained with either biotinylated rat anti–mouse interleukin 12 (IL-12)p40/p70 (clone C17.8 or 15.6) or biotinylated rat anti-mouse CD40 (clone 3/23) for 1 hour. After 3 further washes with FWB, cells were stained with R-PE conjugated rat anti–mouse CD8α (Ly2) (clone 53-6.7) and FITC-conjugated hamster anti–mouse CD11c (clone HL3), as well as Streptavidin-Cychrome (BD Pharmingen, San Diego, CA). After gating on live cells, events (not < 300 000) were collected on a FACScan cytometer (Becton Dickinson, Mountain View, CA) and analyzed using FlowJo software (Treestar, San Carlos, CA).

Results

WASp-null BMDCs exhibit migratory defects in vitro

The inability of human DCs derived from patients with WAS to form podosomes and their failure to migrate effectively have been reported previously.[13,28] The actin cytoskeleton, determined by staining of BMDCs with rhodamine phalloidin, was morphologically similar to that of human WASp-null DCs, and podosomes were not formed (Siobhán Burns and A.J.T., unpublished observations, February 2001). The immunophenotype of WASp-null immature BMDCs was the same as that of control cells (Figure 1). Time-lapse video microscopy showed that immature BMDCs derived from control mice moved rapidly across a fibronectin (FN)–coated surface. The BMDCs polarized, formed a clear leading edge, and established transient but stable contact at this end (Figure 2A and supplemental movie 1A). This was followed by retraction of the trailing edge and net forward motion. In contrast, WASp-null BMDCs failed to establish a dominant leading edge and were unable to detach appropriately (Figure 2A and supplemental movie 1B). This resulted in the formation of a relatively static hyperextended cell morphology, oscillation of the cell body between each pole, and restricted translocation (Figure 2B). Therefore, WASp-null murine DCs exhibit a cytoskeletal phenotype in vitro identical to that observed in mutant human cells and are indicative of significant migratory defects.

Impaired response to CCL21 in vitro

DCs homing to the LN from the skin and within lymphoid tissue are known to involve the up-regulation of chemokine receptor

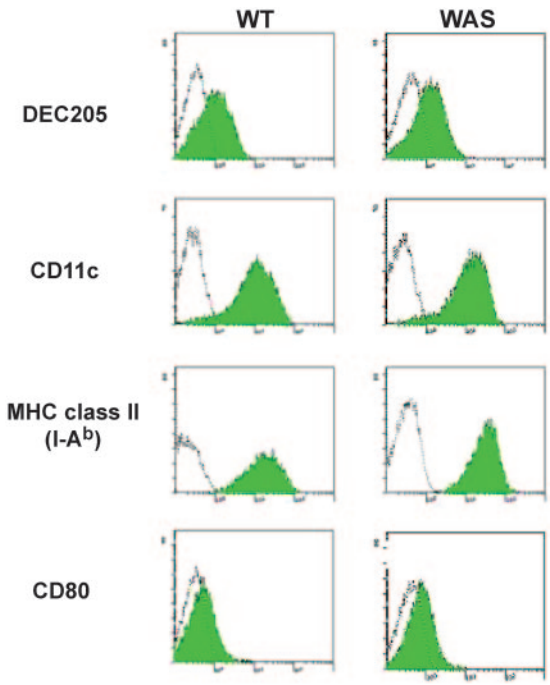

Figure 1. Surface marker expression is normal in WASp-null BMDCs. Unfilled histograms represent either an isotype or second-layer control. Filled histograms show specific expression. WT indicates wild type; WAS, WASp-null BMDCs.

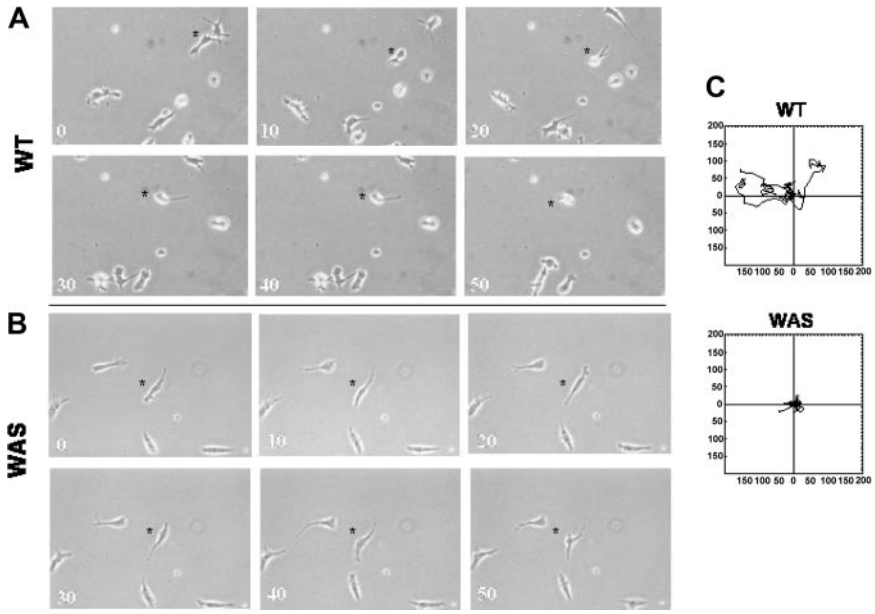

Figure 2. DCs derived from WASp-null mice show a defect in random motility in complete medium (CM) in vitro. Immature BMDCs derived from control sv129 (wild-type [WT]) (A) and WASp-null (WAS) (B) mice were allowed to adhere to fibronectin-coated coverslips before analysis in a Dunn chamber. Cell movement was recorded over 300 minutes using time-lapse microscopy with frames taken at 10-minute intervals (original magnification, × 200). Parallel still images are shown of the first 50 minutes and represent the defective movement of WASp-null BMDCs (the full movie is available as supplemental movie 1A-B at the *Blood* website; see the Supplemental Movies link at the top of the online article). (C) Cell tracks collected using Kinetic Imaging and further analyzed using Mathematica notebook to generate data on the cell trajectories. Migration of WASp-null BMDCs was significantly impaired ($P < .005$, Student *t* test).

CCR7 and for responsiveness to the CCR7 ligands, CCL21 and CCL19. Specifically, CCL21 is expressed on high endothelial venules (HEVs), by stromal cells within T-cell zones, and on lymphatic endothelium.[40] The chemokinetic response of WASp-null DCs to CCL21 was therefore tested in vitro. BMDCs that had been matured overnight with LPS (to render them responsive to CCL21), plated on to FN-coated coverslips, were filmed over a 5-hour period in a Dunn chamber. Maturation of normal and WASp-deficient cells determined by up-regulation of CD80, CD86, major histocompatibility complex (MHC) class II was similar (data not shown). As expected, LPS-matured DCs derived from both normal and WASp-null animals migrated minimally in CM medium alone.[4] In the presence of CCL21, normal BMDCs increased their speed and distance traveled from their origin, while WASp-null cells were significantly less motile (particularly in terms of persistence of migration) over this time period (Figure 3A, and supplemental movie 2A-D). The deficiency of migration could not be accounted for by differences in CCR7 expression, as these were shown to be equivalent both at the level of mRNA (quantitative PCR, data not shown) and surface protein (Figure 3B). Interestingly, the velocity of normal cells to CCL21 is comparable to that observed during contact between primed DCs and T cells in the LN in vivo using the 2-photon microscopy model.[41]

Delayed migration of WASp-null–deficient DCs from the skin to the draining LN

Migration of DCs is important during exit from peripheral tissues, where they enter lymphatics and eventually reach draining lymphoid tissue. To test the hypothesis that DC migration from peripheral sites is compromised in the absence of WASp in vivo, the abdominal skin of normal and mutant mice was sensitized with FITC, and the draining LNs were sampled at subsequent time points. FITC-bearing DCs were identified by flow cytometry using anti–I-A^b following magnetic bead depletion of B and T cells. At 4 hours after sensitization a population of I-A^{b+}FITC$^+$ cells could be detected in normal LNs (Figure 4A), and this was found to be significantly higher compared with that in WASp-null nodes ($P < .05$, Mann-Whitney test) (Figure 4B). By 18 hours a population of I-A^{b+}FITC$^+$ cells was identified consistently in normal nodes in all experiments (Figure 4A). This was not always seen in WASp-null mice, where in some experiments the population of WASp-null I-A^{b+}FITC$^+$ cells in the LN remained reduced at 18 hours (Figure 4B). However, in the remaining (~ 60%) of the experiments WASp-null I-A^{b+}FITC$^+$ migrants were found in similar levels to those seen in the normal mice, so that overall the differences were not significant (Figure 4B). These results indicate that the homing response of DCs lacking WASp is impaired at early time points, resulting in reduced numbers of cells reaching the draining lymphoid tissue following peripheral stimulation, and that this lag period of migration can sometimes persist for as much as 18 hours.

In the course of these experiments it was noted that LNs from normal animals responded to challenge by increase in size and cellularity, whereas WASp-null LNs remained relatively unchanged (not shown). The increase in size presumably reflects direct modulation of the kinetics of lymphocyte traffic and production of inflammatory cytokines by migrating DCs as has been shown previously.[42,43] These findings are reminiscent of the response to injection of CCR7$^+$ normal DCs, which induce LN congestion, and CCR7$^-$ DCs, which fail to migrate to the LN and do not cause congestion.[43] Therefore, abrogated migration of WASp-null DCs to the lymphatics may reflect a reduced response to the CCR7 ligand CCL21, as observed in vitro.

Diminished migration of WASp-null LCs after contact sensitization

To exclude the possibility that reduced migration of FITC-labeled DCs to regional LNs reflected a quantitative deficiency of peripheral LCs, the number of class II–positive cells in the epidermis was determined by immunohistochemistry. The density of I-Ab^+ LCs in the skin of normal and WASp-null mice was comparable (sv129 control, 815 ± 104 LC/mm^2; WASp-null, 821 ± 96 LC/mm^2; Figure 5A), indicating that the steady-state maintenance of LCs in skin, which is dependent on self-renewal, is not compromised quantitatively in the absence of WASp.[44] Next, we investigated whether a contribution to the reduction in DC traffic in WASp-null mice was caused by an inability of adequate numbers of LCs to emigrate from the epidermis. Normal and WASp-null mice were sensitized with oxazolone, and the density of LCs in the epidermis was again determined. Previous studies have shown that the greatest reduction in epidermal LCs occurs at 4 hours.[39,45] In this study, 4 hours after application of oxazolone there was an expected

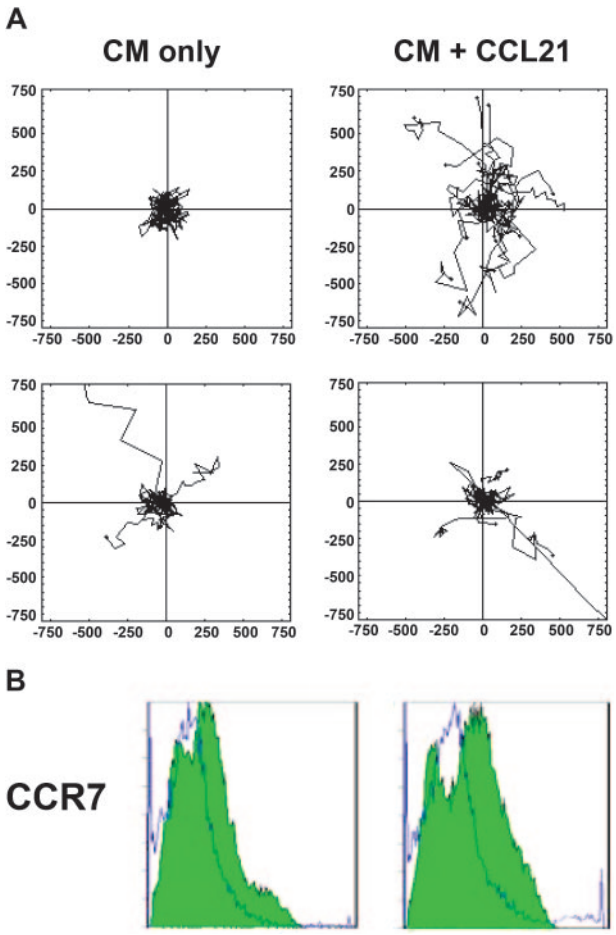

Figure 3. Decreased motility by WASp-null BMDCs in response to CCL21. (A) Control and WASp-null DCs were exposed to 100 ng/mL CCL21, and their migration was followed by time-lapse microscopy for 5 hours. Data on cell tracks were collected using Openlab software and further analyzed using a Mathematica notebook to generate data on cell trajectories and cell speed. In the absence of chemokine (CM), little persistent movement was observed in either control (top row) or WASp-null (bottom row) LPS-matured DCs (mean cell speed = 0.073 ± 0.0076 μm/sec and 0.072 ± 0.013 μm/sec, respectively; mean distance traveled = 1314 ± 137 μm and 858 ± 97 μm, respectively; not significant, $P > .05$). Stimulation with CCL21 (CM + CCL21) dramatically increased both the speed of movement and the persistence of directional migration in control cells, whereas WASp-null DCs failed to migrate effectively (mean cell speed = 0.119 ± 0.0082 μm/sec and 0.076 ± 0.013 μm/sec, respectively; mean distance traveled 2143 ± 145 μm and 1031 ± 110 μm, $P < .01$). Occasional poorly adhered cells, which moved out of the frame, were excluded from the analysis. The cell tracks from 1 of 2 separate experiments were merged into a single file for analysis, giving a total of 22 to 25 cells per treatment. The x- and y-axes are scaled in micrometers (μm). Statistical differences in migration were calculated using a Student *t* test. (See also supplemental movie 2A-D). (B) Levels of CCR7 expression in matured cells from control (left) and WASp-deficient (right) animals were equivalent when measured by flow cytometry. Unfilled histograms represent an isotype control. Filled histograms indicate specific expression.

loss of LCs from the epidermis of normal ears. In contrast, levels of WASp-null LCs remained unchanged compared with those of vector (acetone and olive oil [AOO])–treated ears (Figure 5A). In normal mice there was a significant decline in LC frequency in sensitized skin compared with vector-treated skin (from 836 ± 107 LC/mm^2 to 535 ± 71 LC/mm^2; $P < .001$; Student *t* test) (Figure 5B). Sensitized LC frequencies in normal mice were also significantly lower compared with those of WASp-null mice ($P < .005$; Student *t* test). LC numbers in WASp-null epidermal sheets were not significantly different from those that had been treated with vector alone (from 855 ± 101 LC/mm^2 to 761 ± 101 LC/mm^2; Student *t* test) (Figure 5B). These findings indicate that at least a component of reduced migration to draining lymphoid tissue is due to compromised emigration from peripheral sentinel sites but does not exclude a contribution from defects in traffic through the lymphatics and entry into LNs.

Incomplete localization of WASp-null DCs to splenic T-cell areas

DCs are also mobilized within lymphoid tissue in vivo during an immune response to systemic antigen. This response was examined by intraperitoneal challenge with microbial agents, STAg or LPS, that are known to drain into the spleen and stimulate immature interdigitating DCs to migrate exclusively within the T-cell zone and to form tight clusters.[32,46] Having established that the distribution of interdigitating DCs in unstimulated WASp-null spleen was normal, the mice were challenged with the microbial stimuli. DCs from both normal and WASp-null mice were found to redistribute 6 hours after injection of STAg, forming clusters in T-cell areas (Figure 6A). However, in contrast with the normal spleens, in WASp-null spleens a higher proportion of DCs were retained ectopically in the marginal zone (MZ), suggesting that there was

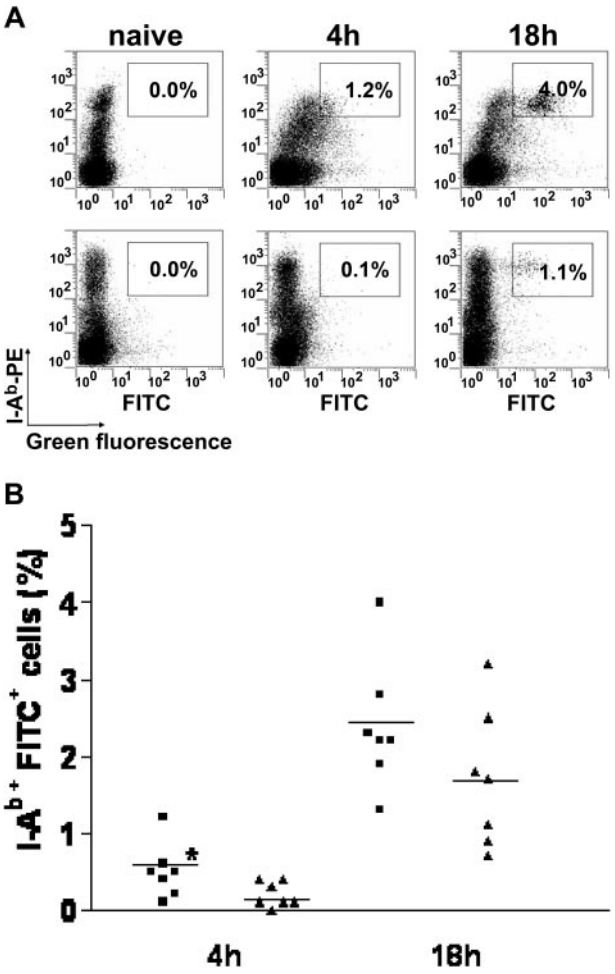

Figure 4. Impaired migration of WASp-null skin DCs to LNs following contact sensitization with FITC. Normal and WASp-null mice were painted with FITC, after which single-cell suspensions of draining LNs were prepared at 4 hours and 18 hours before analysis by flow cytometry. (A) Flow cytometry detects, 4 hours after sensitization, a small but higher percentage of I-A^{b+}/FITC$^+$ cells (right quadrant) in normal (WT, top row) compared with mutant (WASp-null, bottom row) LNs. Consistently, at 18 hours after sensitization, a higher number of I-A^{b+}/FITC$^+$ cells (right quadrant) are found in normal LNs; in contrast, WASp-null I-A^{b+}/FITC$^+$ showed a more variable response. The identity of a small population of I-A^{b-}/FITC$^+$ cells was not determined. This panel represents 1 experiment of 7. (B) Chart shows pooled data of 7 experiments for each group, where each symbol represents a single mouse. A greater percentage of I-A^{b+}/FITC$^+$ immigrants was found in normal (WT, ■) compared with mutant (WASp-null, ▲) LNs (*$P < .05$; Mann-Whitney test) at 4 hours after sensitization only. Horizontal bars indicate the mean.

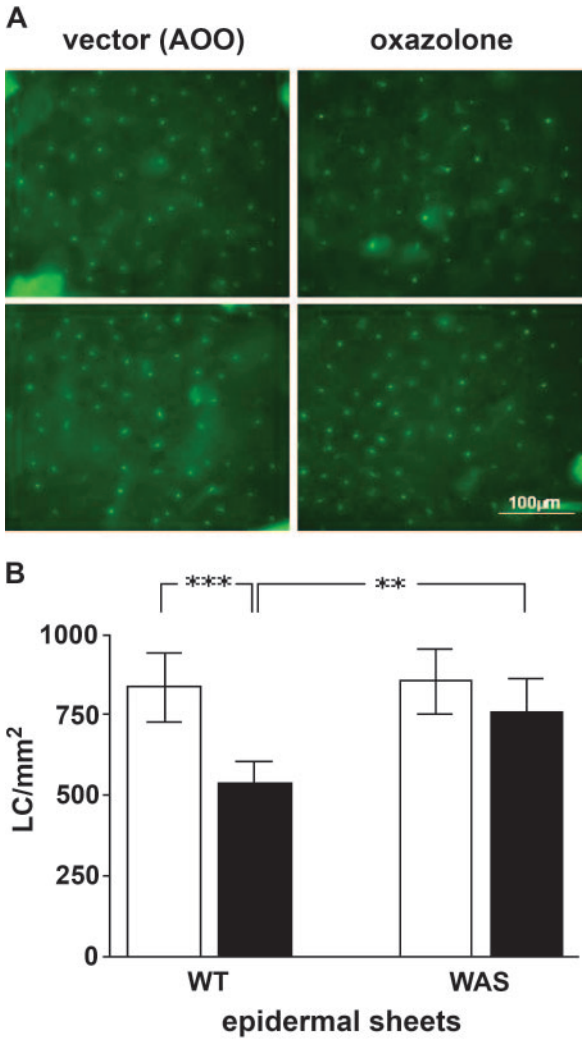

Figure 5. Migration of WASp-null LCs out of the epidermis is diminished. (A) Epidermal sheets were prepared following topical application of 0.1% oxazolone in AOO (acetone and olive oil) or AOO alone (vector). Staining with I-A^{b+}–FITC identified LCs and revealed fewer numbers of these cells in normal animals that had been sensitized compared with those treated with vector alone. In contrast, LC numbers in WASp-null sensitized animals were comparable in number to untreated animals. Top row, WT cells; bottom row, WASp-null. (B) Chart LC frequency in epidermal sheets prepared following topical application of 0.1% oxazolone in AOO (■) or of AOO alone (vector, □). Oxazolone resulted in a marked fall in LC density compared with vector-treated WT mice (***$P < .001$; Student t test). This drop in LC density was also greater in normal compared with WASp-null sensitized animals (**$P < .005$). Additionally LC numbers from oxazolone-treated WASp-null mice did not vary significantly from vector-treated animals. The data shown are representative of 2 experiments in which n = 3 mice. Error bars indicate standard deviation.

incomplete mobilization to the T-cell zones (Figure 6B). Similar abnormalities of DC migration were observed following administration of LPS (Figure 6B).

Mobilization of DCs in response to challenge has been shown to coincide with increased expression of CD40 and production of high levels of IL-12.[32] As expected, following administration of STAg, CD8α$^+$ DCs from control mice upregulated expression of CD40 and secreted IL-12p40/p70 (Figure 7). DCs from WASp-null mice showed similar patterns of activation, indicating that these processes are largely independent of WASp. In addition, overnight culture of 10^5 splenocytes from STAg-primed mice revealed no significant difference in the levels of IL-12p40/p70 compared with splenocytes from control mice as measured by enzyme-linked immunosorbent assay (ELISA; data not shown).

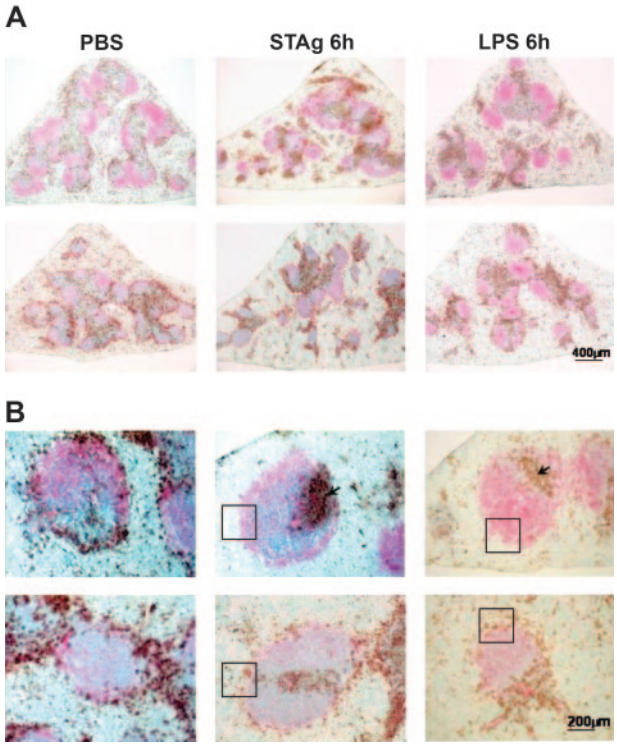

Figure 6. WASp-null CD11c$^+$ DCs are able to redistribute from red pulp and the marginal zone of the white pulp to the T-cell zone after challenge with STAg or LPS, although some DCs remain in the marginal zone. Spleens from control sv129 (WT) and WASp-null mice were challenged with PBS, STAg, and LPS and analyzed 6 hours after injection. The sections were stained for CD11c (brown) and CD19 (pink) to delineate the follicles in the white pulp and analyzed. (A) The splenic microarchitecture in the WASp-null mice (bottom row) was observed to be somewhat disfigured compared with control mice (top row). At low power, "nests" of DCs in T-cell areas are clearly visible in both mice (scale bar represents 400 μm). (B) Higher-power images indicate the presence of CD11c$^+$ cells exclusively in T-cell areas (arrow) in normal spleen (top row) after challenge with STAg or LPS. However, in WASp-null spleen (bottom row) a proportion of CD11c$^+$ cells is retained in the marginal zone (highlighted in boxed areas) (scale bar represents 200 μm). The STAg challenge data shown are representative of 3 experiments, and LPS challenge data represent 1 experiment with triplicate samples.

A confounding observation was that the splenic architecture of WASp-null animals (maintained in a sterile environment) was morphologically distinct from that of control animals with respect to several features. WASp-null mice often exhibited splenomegaly, and, although B- and T-cell segregation was observed, the white pulp was spatially disorganized and unevenly distributed (see

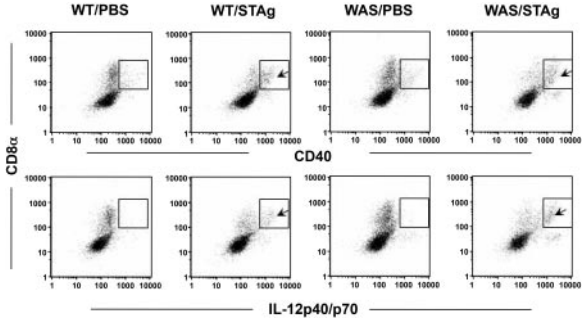

Figure 7. IL-12p40 is produced at similar levels by normal (WT) and WASp-null (WAS) CD11c$^+$CD8α$^+$ DCs in response to STAg 6 hours after injection. Arrows indicate the gated CD11c$^+$ splenocytes expressing CD40 or IL-12 after STAg challenge; this expression is absent in PBS-treated spleens. An isotype-matched rat IgG2a control antibody produced a staining pattern identical to that seen with the PBS control (data not shown). Data presented are from 1 of 2 independent experiments with similar results.

Figure 3A), forming larger aggregates that are normally seen on equivalent transverse sections. A narrower marginal zone with marked depletion of MZ B cells was also noted (not shown), similar to that seen in human splenic tissue from patients with WAS.[47] These abnormal features could compromise appropriate localization of WASp-null interdigitating DCs to T-cell areas, although WASp-null primary (immature) splenic DCs sorted for $CD11c^+$ and $I\text{-}A^{b+}$ expression by FACS ($\geq$ 98% purity) displayed defective motility on FNs similar to that observed for BMDCs (data not shown). We conclude therefore that migration of mutant CD8α splenic DCs is compromised as a result of intrinsic cytoskeletal defects, but that activation can be initiated normally.

Discussion

In this study we have shown that WASp-null DCs exhibit defects of cell migration at multiple levels in vivo, including emigration from skin, trafficking to draining LNs, and spatial localization within the LNs. There are clearly many ways in which these defects could contribute to immune dysregulation. Inefficient delivery of antigen to lymphoid tissue would compromise the development of physiologic immune responses, and activation without migration to a regulated microenvironment could result in the initiation or propagation of ectopic inflammatory processes. The maintenance of tolerance, and the homeostatic regulation of naive and memory T-cell populations, which require varying degrees of interaction between MHC and T-cell receptor (TCR) to preserve numbers and function, might therefore also be disturbed.[48] As shown in this study, the defects of cell migration in vivo are not absolute, and proper localization may be achieved over time. However, the requirement for coordinated interaction (both temporal and spatial) between antigen, immune cells such as DCs and T cells, and their microenvironment would predict that subtle aberrations might well be sufficient to dysregulate normal immune mechanisms. Contributions from intrinsically defective TCR signaling or T-cell trafficking are also probable and will require the development of lineage-specific murine models of WASp deficiency in order to be evaluated fully.

Abnormalities of WASp-null DC migration, which previously have been described in human cells, are as shown here, mirrored in murine cells. The underlying cellular mechanisms are probably multiple but relate to the defective function of the actin cytoskeleton. It is likely that mutant DCs are defective for chemotaxis (the directional response to stimuli) as has been observed in macrophages.[27,29] This reflects defective polarization and formation of filopodia, which are necessary for a normal chemotactic response as demonstrated by inhibition of Cdc42 in a Bac1 macrophage cell line.[37] However, the quality of migration of WASp-null DCs is also highly disturbed, both in terms of development of a dominant leading edge and retraction of the tail. This is indicative of defects in protrusive activity and in the dynamics of adhesion. Unsurprisingly, many aspects are mimicked by inhibition of Rho GTPases by *Clostridium difficile* toxin B.[15] The absence of podosomes may contribute significantly to the inability of cells such as DCs and macrophages to rapidly attach and detach from substrata. The formation of these structures is regulated in a concerted way by Cdc42, Rac, and RhoA but is absolutely dependent on WASp.[14] Maturation of DCs is associated with the disappearance of podosomes within 2 to 4 hours, suggesting that they are important early on in the migratory process of peripheral DCs on the way to draining secondary lymphoid tissue.[19] The concentrated expression of the β2-family of integrins on DC podosomes also suggests that a key function is for diapedesis, including entry or exit from the lymphatic system through interaction with molecules such as ICAM-1 or JAM-A.

Together, abnormalities of DC migration, and of migration of T and B lymphocytes, are likely to be responsible for the observed disorganization of microarchitecture in the lymphoid tissues of WASp-null animals. There is some resemblance to the findings in CCR7-deficient animals, where failure of lymphocyte and DC migration leads to profound abnormalities in the microarchitecture of all secondary lymphoid tissue.[49] CCR7 is responsible for migration of DCs to lymphatics and is up-regulated following activation.[50] The ligands for CCR7 are CCL19, expressed by stromal cells and mature DCs in T-cell areas, and CCL21, expressed by lymphatic endothelial cells. Unsurprisingly, therefore, DCs from CCR7-null mice, although able to activate normally in vitro, fail to migrate to draining LNs[49] and also fail to induce changes in the kinetics of lymphocyte traffic that normally result in LN congestion after DC migration.[43] Defects of DC accumulation in T-cell zones have also been demonstrated in *plt/plt* mice that are functionally deficient in both CCL19 and CCL21.[51] CCR7 has also recently been shown to be a key regulator of DC migration into afferent dermal lymphatics under inflammatory and steady-state conditions, suggesting an important role for maintenance of peripheral tolerance as well as for generation of protective immunity.[52] As shown in this study, WASp-null DCs exhibit a reduced response to CCL21 and also defective homing to lymph nodes. We also noted that the kinetics of lymphocyte traffic after contact sensitization was not normally increased in WASp-null animals. Although not conclusive, it is likely that these observations are directly linked. It is also likely that WASp-null DCs are compromised in their ability to respond to other specific chemokinetic stimuli, eg, during clustering in T-cell areas after challenge with systemic microbial antigen, although this has not yet been investigated in detail. The contribution of abnormal DC trafficking to the immunodeficiency (and breakdown of tolerance) in the WAS is difficult to ascertain because of deficiencies in multiple immune cell lineages. The development of lineage-restricted WASp-deficient models may be useful in this context. Likewise, CCR7 mediates trafficking of both DCs and lymphocytes, and, although a direct parallel cannot be drawn between WASp deficiency and CCR7 deficiency, the delayed antibody responses and delayed-type hypersensitivity (DTH) reactions that have been observed in both models could arise (at least in part) from similar trafficking defects.

In summary, we have demonstrated in this study that WASp is a key molecule for the regulated migration and trafficking of DCs in vivo and suggest that defects in this process may promote abnormalities of immune response and maintenance of tolerance. We also suggest that disturbances of immune cell trafficking, including DCs, are likely to provide an explanation for many of the immunologic abnormalities of the WAS.

Acknowledgments

We would like to thank Deborah Aubyn from the Light Microscopy Laboratory (CRUK) and Siobhan Burns (Molecular Immunology, ICH) for their assistance.

References

1. Banchereau J, Steinman RM. Dendritic cells and the control of immunity. Nature. 1998;392:245-252.
2. Banchereau J, Briere F, Caux C, et al. Immunobiology of dendritic cells. Annu Rev Immunol. 2000; 18:767-811.
3. Dieu MC, Vanbervliet B, Vicari A, et al. Selective recruitment of immature and mature dendritic cells by distinct chemokines expressed in different anatomic sites. J Exp Med. 1998;188:373-386.
4. Lin CL, Suri RM, Rahdon RA, Austyn JM, Roake JA. Dendritic cell chemotaxis and transendothelial migration are induced by distinct chemokines and are regulated on maturation. Eur J Immunol. 1998;28:4114-4122.
5. Sozzani S, Allavena P, D'Amico G, et al. Differential regulation of chemokine receptors during dendritic cell maturation: a model for their trafficking properties. J Immunol. 1998;161:1083-1086.
6. Sallusto F, Schaerli P, Loetscher P, et al. Rapid and co-ordinated switch in chemokine receptor expression during dendritic cell maturation. Eur J Immunol. 1998;28:2760-2769.
7. Chan VW, Kothakota S, Rohan MC, et al. Secondary lymphoid-tissue chemokine (SLC) is chemotactic for mature dendritic cells. Blood. 1999; 93:3610-3616.
8. Jones GE. Cellular signaling in macrophage migration and chemotaxis. J Leukoc Biol. 2000;68: 593-602.
9. Etienne-Manneville S, Hall A. Rho GTPases in cell biology. Nature. 2000;420:629-635.
10. Thrasher AJ. WASp in immune-system organization and function. Nat Rev Immunol. 2002;2:635-646.
11. Badour K, Zhang J, Shi F, et al. The Wiskott-Aldrich syndrome protein acts downstream of CD2 and the CD2AP and PSTPIP1 adaptors to promote formation of the immunological synapse. Immunity. 2003;18:141-154.
12. Notarangelo LD, Ochs HD. Wiskott-Aldrich Syndrome: a model for defective actin reorganization, cell trafficking and synapse formation. Curr Opin Immunol. 2003;15:585-591.
13. Linder S, Nelson D, Weiss M, Aepfelbacher M. Wiskott-Aldrich syndrome protein regulates podosomes in primary human macrophages. Proc Natl Acad Sci U S A. 1999;96:9648-9653.
14. Burns S, Thrasher AJ, Blundell MP, Machesky L, Jones GE. Configuration of human dendritic cell cytoskeleton by Rho GTPases, the WAS protein, and differentiation. Blood. 2001;98:1142-1149.
15. Swetman CA, Leverrier Y, Garg R, et al. Extension, retraction and contraction in the formation of a dendritic cell dendrite: distinct roles for Rho GTPases. Eur J Immunol. 2002;32:2074-2083.
16. Calle Y, Jones GE, Jagger C, et al. WASp deficiency in mice results in failure to form osteoclast sealing zones and defects in bone resorption. Blood. 2004;103:3552-3561.
17. Martin-Padura I, Lostaglio S, Schneemann M, et al. Junctional adhesion molecule, a novel member of the immunoglobulin superfamily that distributes at intercellular junctions and modulates monocyte transmigration. J Cell Biol. 1998;142: 117-127.
18. Ostermann G, Weber KS, Zernecke A, Schroder A, Weber C. JAM-1 is a ligand of the beta(2) integrin LFA-1 involved in transendothelial migration of leukocytes. Nat Immunol. 2002;3:151-158.
19. Burns S, Hardy SJ, Buddle J, Yong KL, Jones GE, Thrasher AJ. Maturation of DC is associated with changes in motile characteristics and adherence. Cell Motil Cytoskeleton. 2004;57:118-132.
20. Molina IJ, Sancho J, Terhorst C, Rosen FS, Remold-O'Donnell E. T cells of patients with the Wiskott-Aldrich syndrome have a restricted defect in proliferative responses. J Immunol. 1993; 151:4383-4390.
21. Snapper SB, Rosen FS, Mizoguchi E, et al. Wiskott-Aldrich syndrome protein-deficient mice reveal a role for WASP in T but not B cell activation. Immunity. 1998;9:81-91.
22. Zhang J, Shehabeldin A, da Cruz LA, et al. Antigen receptor-induced activation and cytoskeletal rearrangement are impaired in Wiskott-Aldrich syndrome protein-deficient lymphocytes. J Exp Med. 1999;190:1329-1342.
23. Lorenzi R, Brickell PM, Katz DR, Kinnon C, Thrasher AJ. Wiskott-Aldrich syndrome protein is necessary for efficient IgG-mediated phagocytosis. Blood. 2000;95:2943-2946.
24. Badour K, Zhang J, Shi F, Leng Y, Collins M, Siminovitch KA. Fyn and PTP-PEST-mediated regulation of Wiskott-Aldrich Syndrome protein (WASp) tyrosine phosphorylation is required for coupling T cell antigen receptor engagement to WASp effector function and T cell activation. J Exp Med. 2004;199:99-112.
25. Dupre L, Aiuti A, Trifari S, et al. Wiskott-Aldrich syndrome protein regulates lipid raft dynamics during immunological synapse formation. Immunity. 2002;17:157-166.
26. Sasahara Y, Rachid R, Byrne MJ, et al. Mechanism of recruitment of WASP to the immunological synapse and of its activation following TCR ligation. Mol Cell. 2002;10:1269-1281.
27. Badolato R, Sozzani S, Malacarne F, et al. Monocytes from Wiskott-Aldrich patients display reduced chemotaxis and lack of cell polarization in response to monocyte chemoattractant protein-1 and formyl-methionyl-leucyl-phenylalanine. J Immunol. 1998;161:1026-1033.
28. Binks M, Jones GE, Brickell PM, Kinnon C, Katz DR, Thrasher AJ. Intrinsic dendritic cell abnormalities in Wiskott-Aldrich syndrome. Eur J Immunol. 1998;28:3259-3267.
29. Zicha, D, Allen WE, Brickell PM, et al. Chemotaxis of macrophages is abolished in the Wiskott-Aldrich syndrome. Br J Haematol. 1998;101:659-665.
30. Haddad E, Zugaza JL, Louache F, et al. The interaction between Cdc42 and WASP is required for SDF-1–induced T-lymphocyte chemotaxis. Blood. 2001;97:33-38.
31. Lacout C, Haddad E, Sabri S, et al. A defect in hematopoietic stem cell migration explains the nonrandom X-chromosome inactivation in carriers of Wiskott-Aldrich syndrome. Blood. 2003; 102:1282-1289.
32. Reis E, Sousa C, Hieny S, et al. In vivo microbial stimulation induces rapid CD40 ligand-independent production of interleukin 12 by dendritic cells and their redistribution to T cell areas. J Exp Med. 1997;186:1819-1829.
33. Inaba K, Inaba M, Romani N, et al. Generation of large numbers of dendritic cells from mouse bone marrow cultures supplemented with granulocyte/macrophage colony-stimulating factor. J Exp Med. 1992;176:1693-1702.
34. Zal T, Volkmann A, Stockinger B. Mechanisms of tolerance induction in major histocompatibility complex class II-restricted T cells specific for a blood-borne self-antigen. J Exp Med. 1994;180: 2089-2099.
35. Ritter U, Wiede F, Mielenz D, Kiafard Z, Zwirner J, Korner H. Analysis of the CCR7 expression on murine bone marrow-derived and spleen dendritic cells. J Leukoc Biol. 2004;76:472-476.
36. Zicha D, Dunn GA, Brown AF. A new direct-viewing chemotaxis chamber. J Cell Sci. 1991; 99:769-775.
37. Allen WE, Zicha D, Ridley AJ, Jones GE. A role for Cdc42 in macrophage chemotaxis. J Cell Biol. 1998;141:1147-1157.
38. Cumberbatch M, Kimber I. Phenotypic characteristics of antigen-bearing cells in the draining lymph nodes of contact sensitized mice. Immunology. 1990;71:404-410.
39. Antonopoulos C, Cumberbatch M, Dearman RJ, Daniel RJ, Kimber I, Groves RW. Functional caspase-1 is required for Langerhans cell migration and optimal contact sensitization in mice. J Immunol. 2001;166:3672-3677.
40. von Andrian UH, Mempel TR. Homing and cellular traffic in lymph nodes. Nat Rev Immunol. 2003;3:867-878.
41. Mempel TR, Henrickson SE, von Andrian UH. T-cell priming by dendritic cells in lymph nodes occurs in three distinct phases. Nature. 2004;427: 154-159.
42. Mandala S, Hajdu R, Bergstrom J, et al. Alteration of lymphocyte trafficking by sphingosine-1-phosphate receptor agonists. Science. 2002;296:346-349.
43. Martin-Fontecha A, Sebastiani S, Hopken UE, et al. Regulation of dendritic cell migration to the draining lymph node: impact on T lymphocyte traffic and priming. J Exp Med. 2003;198:615-621.
44. Merad M, Manz MG, Karsunky H, et al. Langerhans cells renew in the skin throughout life under steady-state conditions. Nat Immunol. 2002;3: 1135-1141.
45. Xu H, Guan H, Zu G, et al. The role of ICAM-1 molecule in the migration of Langerhans cells in the skin and regional lymph node. Eur J Immunol. 2001;31:3085-3093.
46. De Smedt T, Pajak B, Muraille E, et al. Regulation of dendritic cell numbers and maturation by lipopolysaccharide in vivo. J Exp Med. 1996;184: 1413-1424.
47. Vermi W, Blanzuoli L, Kraus MD, et al. The spleen in the Wiskott-Aldrich syndrome: histopathologic abnormalities of the white pulp correlate with the clinical phenotype of the disease. Am J Surg Pathol. 1999;23:182-191.
48. Kassiotis G, Zamoyska R, Stockinger B. Involvement of avidity for major histocompatibility complex in homeostasis of naive and memory T cells. J Exp Med. 2003;197:1007-1016.
49. Forster R, Schubel A, Breitfeld D, et al. CCR7 coordinates the primary immune response by establishing functional microenvironments in secondary lymphoid organs. Cell. 1999;99:23-33.
50. Yanagihara S, Komura E, Nagafune J, Watarai H, Yamaguchi Y. EBI/CCR7 is a new member of dendritic cell chemokine receptor that is up-regulated upon maturation. J Immunol. 1998;161: 3096-3102.
51. Gunn MD, Kyuwa S, Tam C, et al. Mice lacking expression of secondary lymphoid organ chemokine have defects in lymphocyte homing and dendritic cell localization. J Exp Med. 1999;189:451-460.
52. Ohl L, Mohaupt M, Czeloth N, et al. CCR7 governs skin dendritic cell migration under inflammatory and stead-state conditions. Immunity. 2004; 21:279-288.